JOURNAL OF MATERIALS SCIENCE **37** (2002) 133–139

Study on the formation of Pt/C catalysts by non-oxidized active carbon support and a sulfur-based reducing agent

E. ANTOLINI
Scuola di Scienza di Materiali, Via 25 Aprile 22, 16016 Cogoleto (Genova), Italy
E-mail: ermantol@libero.it

F. CARDELLINI, E. GIACOMETTI
ENEA C.R. Casaccia, Erg Tea Echi, Via Anguillarese 301, 00060 Santa Maria di Galeria (Roma), Italy

G. SQUADRITO
CNR ITAE, Salita S. Lucia sopra Contesse 39, Messina, Italy

The formation mechanism of Pt/C catalysts using non-oxidized active carbon support and the weak reducing agent $Na_2S_2O_4$ was investigated. Platinum on carbon catalysts were fabricated by an impregnation/reduction process of the Pt-precursor H_2PtCl_6 on carbon support. The effect of thermal treatment in argon up to 700°C on the structural characteristics of these catalysts was studied by XRD and TEM analyses. The importance of carbon support properties on Pt/C formation was recognized. Before thermal treatment a very weak internal organization (a very small particle size and amorphous structure) in the metal was obtained. Thermal treatment at relatively low temperatures leads to the growth and then to the crystallization of platinum particles in the well-known face centered cubic structure. The sintering of Pt particles occurs through the migration of Pt atoms on the carbon support, likely by a bridge-bonding mechanism on sulfur atoms. A fast growth of Pt particles occurred in the temperature range 300–400°C. Thermal crystallization, instead, occurred mostly going from 400 to 550°C. Following annealing at 550°C, the formation of platinum sulfide was revealed. The sample thermally treated at 700°C showed an anomalous XRD pattern with Pt reflexions shifted towards high angles and an increase of Pt[111]/Pt[220] peak intensity ratio.

1. Introduction

Platinum supported on carbon (Pt/C) is used as catalyst for hydrogenation and oxidation reactions. Pt/C is the best known electrocatalyst for both hydrogen oxidation and oxygen reduction in phosphoric acid fuel cells (PAFCs) and proton exchange membrane fuel cells (PEMFCs). Platinum has a face-centered cubic (fcc) structure. Romanowski [1] found that a minimum surface energy is obtained for Pt particles having a cubo-octahedral structure. The cubo-octahedral particles of unsupported platinum consist of eight octahedral [111] crystal faces and six cubic [100] crystal faces bounded by edge and corner atoms. In general, the shape of the supported clusters is shown to depend on the strength of the metal-support interactions and on the size of the cluster [2–4]. Platinum particle size affects the electrocatalytic activity of highly dispersed Pt for oxygen reduction: some works reported that the mass activity reaches a maximum at about 4 nm [5, 6]. More recently, Kabbabi *et al*. [7] found a loss of catalytic activity with decreasing particle size, particularly for Pt cluster sizes <10 nm. So, it is very important to control the particle size of the metal both during the preparation process and in operating conditions. Many papers deal with Pt particle growth of platinized carbon. Tseung and Dhara [8] and Honji *et al*. [9] studied the loss of surface area of platinum supported on carbon in hot phosphoric acid (150–200°C) at 0.7–0.8 V. They concluded that the dissolution and redeposition of platinum crystallites is the predominant growth mechanism. Platinum particles in a colony were agglomerated to form one particle depending on the potential and the number of particles in the colony [9]. Besides this dissolution/redeposition mechanism, Pt particle growth takes place also in the absence of a liquid environment. The surface diffusion of crystallites or migration of platinum atoms also occurs in gaseous environment, as nitrogen or hydrogen, at temperatures above 600°C [10, 11]. The stability of the metal particles and the mechanism of Pt particle growth depend on the properties of the carbon support. Torre *et al*. [12] studied the influence of surface acid-base properties on the formation of Pt/C catalysts using a high specific surface area carbon. They found that surface acidic oxygen-containing functional groups may

act as anchoring centres for the metal particles limiting their growth in the low temperature range. The progressive decomposition of these acidic surface groups with increasing temperature allows a fast growth of the Pt particles. He *et al.* [13] prepared PtRu/C catalyst by H_2PtCl_6 reduction with sodium thiosulfate and a further reduction in H_2 atmosphere at 250°C. They obtained PtRu crystal particles too small to be detected by XRD analysis. When this catalyst was heat-treated at 660°C in N_2 atmosphere, very strong PtRu reflexions were detected, this behavior being related to metal particle growth. A Pt/C multilayer thermally treated at 500°C showed Pt crystallite growth and a strong texture of platinum in the [220] -plane [14]. Aim of this work is to evaluate the effect of thermal treatment on morphological and structural characteristics of Pt particles and to obtain Pt/C catalyst with improved the catalytic properties.

The catalyst was prepared by an impregnation/reduction process of H_2PtCl_6 into carbon. The chemistry of the impregnation process is still not well understood. Early XPS studies [15] indicated that after impregnation of carbon with H_2PtCl_6 and subsequent drying in air, the platinum was present as Pt^0 and Pt^{2+}. Van Dam *et al.* [16] showed that upon impregnation into activated carbon, H_2PtCl_6 is partly converted into a Pt^{2+} complex. According to de Miguel *et al.* [17], the interaction of H_2PtCl_6 with the carbon implies a redox process in which after impregnation and drying the metal complex is stabilized as Pt^{2+} on the carbon surface. The reduction method commonly used in the preparation of Pt/C catalysts is treatment with H_2 gas at temperatures in the range 300–400°C [18]. In the present work the reduction was performed by the weak reducing agent $Na_2S_2O_4$ [19]. $Na_2S_2O_4$ reacts with the chloroplatinic ions to form finely divided metal particles having a large surface area. It seems that in this reaction much finely divided sulfur may be formed by decomposition of the sulfur-precursor according to the following equation, which is known to occur in an acidic solution:

$$S_2O_4^{2-} + 2H^+ \rightarrow H_2S_2O_4 \rightarrow S + H_2SO_4 \quad (1)$$

The sulfur particles thus obtained serve as nuclei for growing much finely divided metal catalyst particles.

2. Experimental procedure

The catalysts consisting of Pt supported on carbon were prepared by a deposition/reduction process of H_2PtCl_6. The H_2PtCl_6 is first adsorbed on the carbon support, then it is "*in situ*" reduced to metallic Pt. Two carbon supports were used. Vulcan XC-72R Cabot (VC) has a specific surface area of 254 $m^2\,g^{-1}$ and an average primary particle diameter of 30 nm. Generally, before Pt-precursor deposition, the carbon support is activated by nitric acid oxidation to increase the anchoring centres for the platinum. In the present study, to maintain few active sites on the carbon, we have used the carbon support without any oxidation. A Pt supported on Ketjenblack (KJB) type carbon was prepared to evaluate the effect of support characteristics. KJB has a high specific surface area of 900 $m^2\,g^{-1}$ and high basicity (presence of a high concentration of basic functional groups). An aqueous solution (50 ml) of hexachloroplatinic acid (15 mgPt ml^{-1}) was added to a suspension of carbon (250 ml, 10 mgC ml^{-1}) in a water/ethanol mixture (80/20), following by addition of oxygen peroxide (10 ml, 30% H_2O_2). The H_2O_2 added to the solution can react with the carbon surface. The resulting suspension was heated at 60°C (impregnation step). Then an aqueous solution of $Na_2S_2O_4$ was slowly added (reduction step). Finally, the platinized carbon was filtered, washed in H_2O and dried in air at 110°C. The catalyst was also submitted to a dynamic thermal treatment in argon from room temperature to a maximum temperature in the range 200–700°C at heating rate 15°C/min. To evaluate the effect of the heating rate on Pt particle characteristics, the sample thermally treated up to 350°C was also submitted to a heating rate of 45°C/min.

Chemical analysis of the catalyst was accomplished using Atomic Absorption Spectrophotometry (AAS) by a Perkin Elmer Model 305.

X-ray diffraction (XRD) measurements were carried out with a Italstructures powder diffractometer, using a focused and monochromatized Co K_α source, with a position sensitive detection 120°.

The morphology and the platinum particle size distributions of the catalyst were analyzed by a Philips CM12 Transmission Electron Microscope (TEM). The size distribution of supported particles was represented by the number of the particles in each diameter range. The number-average diameter D_n of Pt particles was calculated from the particle size distribution according to the equation $D_n = \Sigma N_i D_i / \Sigma N_i$ where N_i is the

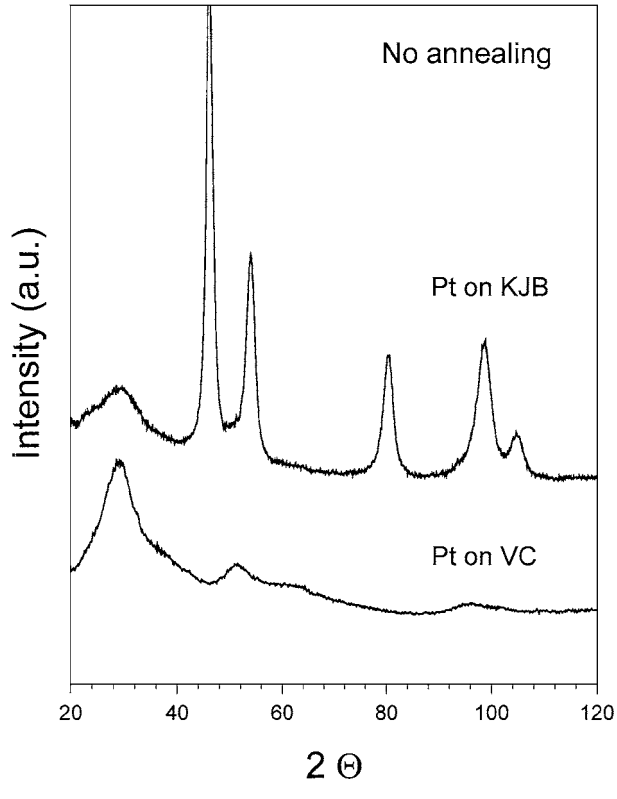

Figure 1 X-ray diffraction patterns of platinum supported on VC (a) and KJB (b) before annealing.

number of particles in a specific size range and D_i is the average diameter in each diameter range.

3. Results and discussion

AAS analysis indicated that metal loading in Pt supported on VC was about 4%, while in Pt supported on KJB was ca. 10%. Fig. 1a shows the XRD pattern of Pt on VC before thermal treatment. Note the absence of Pt reflections. Carbon reflections were only present. Fig. 2a shows a TEM micrograph of the same sample. It was difficult to distinguish Pt particles from the carbon support. Thus the average particle size was smaller than ca. 1.0 nm. The importance of the carbon support characteristics was evidenced by the XRD pattern of Pt supported on KJB. As shown in Fig. 1b, the reflections of well crystallized Pt particles are visible. The different behaviour of the platinum in the presence of different carbon supports can be explained as follows. In the case of non-activated VC, weak carbon surface-metal precursor interactions take place during impregnation, so Pt crystallites nucleate and grow on sulfur particles formed during reduction. Owing to the high number of S particles, the Pt dispersion is high, resulting in small Pt aggregates. In the case of KJB, instead, the presence of basic sites on the carbon surface plays an important role in the adsorption of H_2PtCl_6, by undergoing a strong interaction with it [12]. During reduction the crystallites nucleate and grow on some of these sites. The Pt^{2+} reduction on the crystallite surface being the rate limiting step ($Na_2S_2O_4$ is a weak reducing agent, the Pt^{2+} diffusion is relatively fast), the growth rate of a crystallite will be proportional to its surface area. So, large crystallites will grow faster than small crystallites. This finally results in a small number of large crystallites.

Fig. 3 shows XRD patterns of Pt supported on VC catalysts following thermal treatment. After thermal treatment up to 300°C only the carbon reflections were visible in XRD patterns. Pt reflections appeared starting

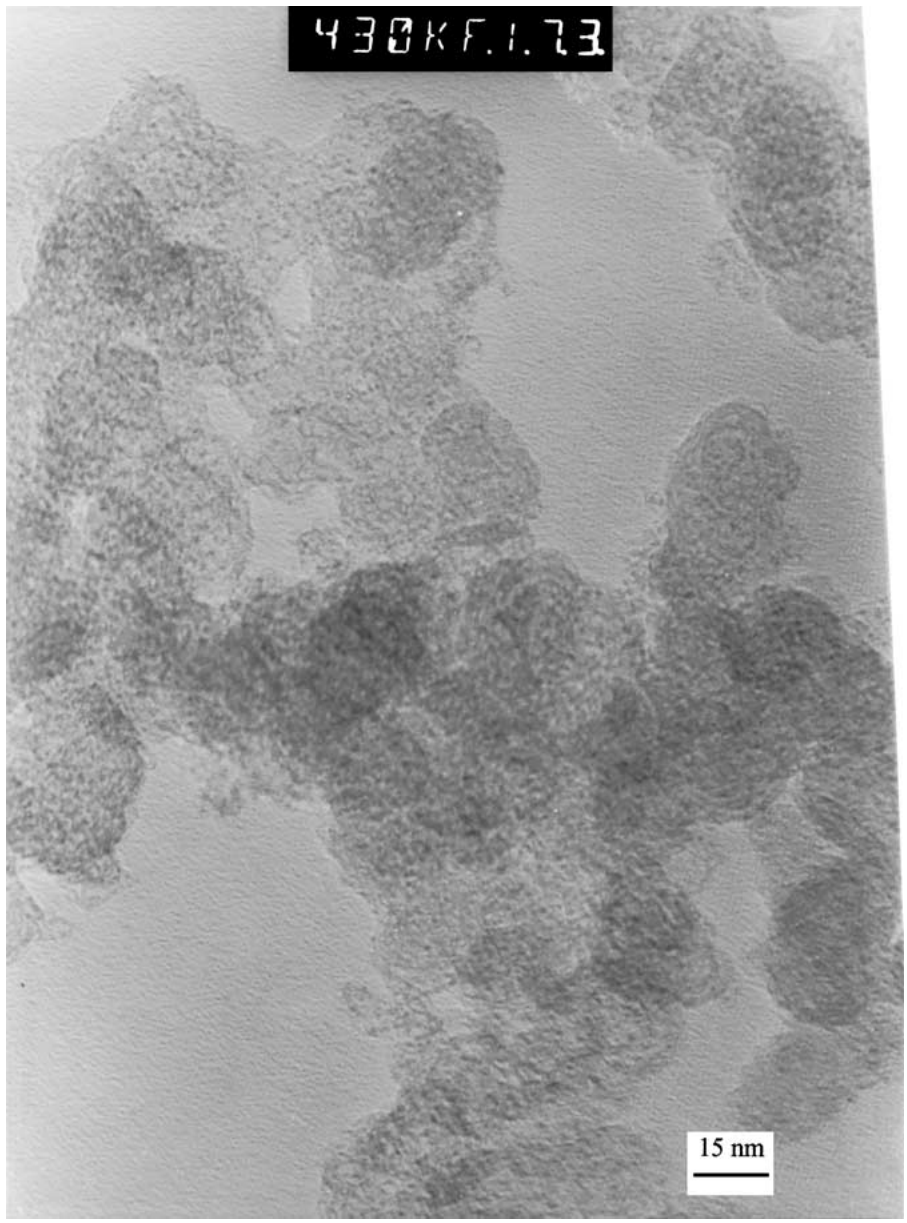

(a)

Figure 2 TEM micrographs of Pt/C on VC catalysts before annealing (a) and following thermal treatment up to 400°C (b) and 700°C (c). (*Continued.*)

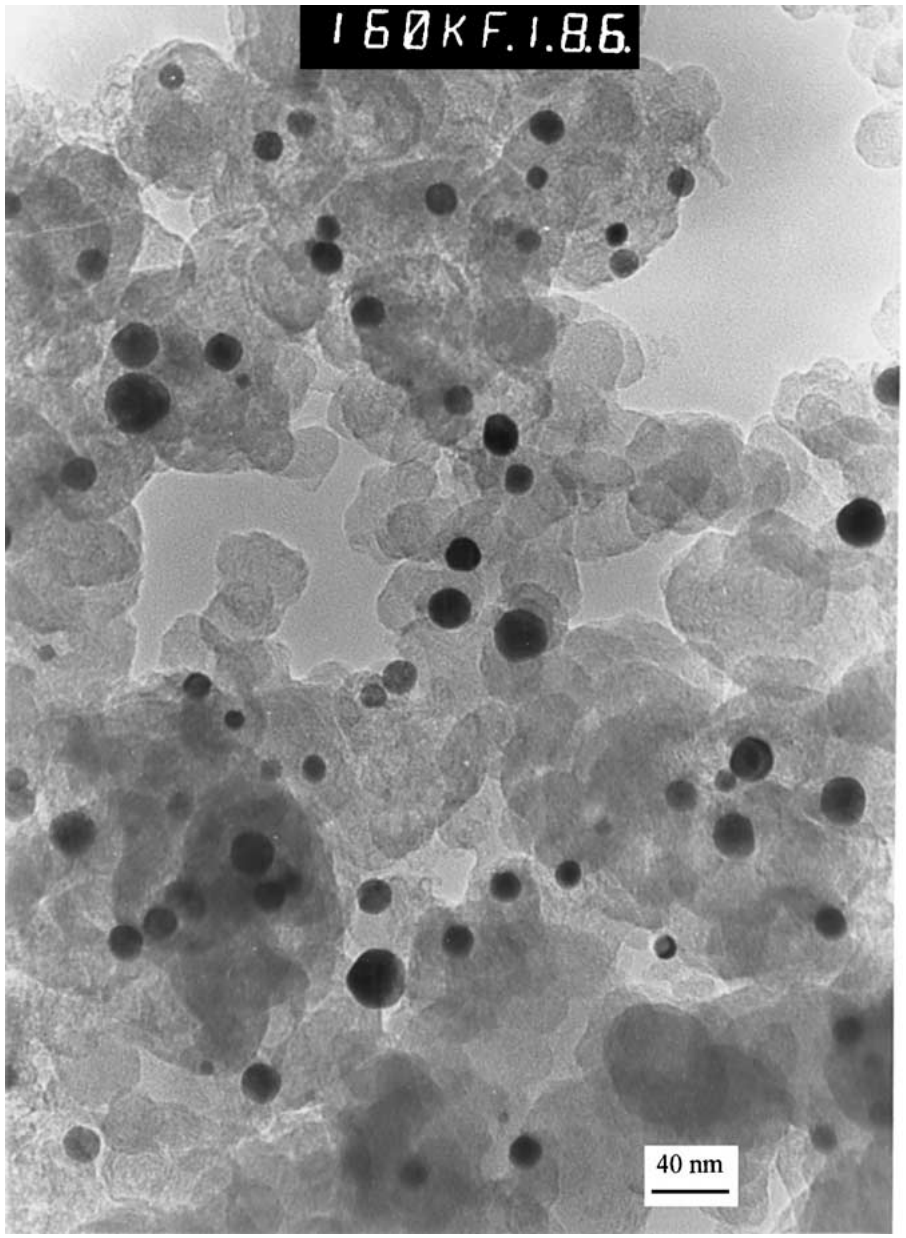

(b)

Figure 2 (*Continued*.)

from thermal treatment up to 350°C. In the XRD pattern following thermal treatment up to 550°C the reflections of PtS (cooperite) were also visible. Both platinum particle growth and thermocrystallization took place during annealing. Particle size D was calculated by XRD measurements from the Scherrers relation:

$$D = k\lambda/2\Delta\theta\cos\theta \qquad (2)$$

where λ is the wave length of x-ray (1.789 Å), θ the angle at the position of the peak maximum, $\Delta\theta$ the width of the diffraction peak at half height, and k is a coefficient taken as 0.9. To aim to discharge the strain of the crystallites, we have used in Equation 2 the extrapolated value of $2\Delta\theta\cos\theta$ at $\theta = 0$, obtained by the plot of $2\Delta\theta\cos\theta$ vs. sen θ. Fig. 4 shows the dependence of particle size on thermal treatment temperature. The coalescence of Pt particles almost completely occurred in the temperature range 300–400°. Sulfur presence can support the sintering of Pt particles at relatively low temperatures, as denoted by an x-ray absorption (XAS) study of Pt clusters in zeolite after poisoning with sulfur [20]. In the presence of sulfur, Pt mobility on carbon takes place by a different route. S enables Pt atoms to move by a bridge-bonding mechanism [21]. TEM analysis of sample annealed up to 400°C confirmed the results of XRD measurements, as shown by comparing the average particle size obtained from both XRD and TEM measurements, reported in Table I. The disagreement of XRD and TEM values of particle size regarding the sample thermally treated up to 700°C can

TABLE I Pt particle size obtained by TEM and XRD measurements before thermal treatment and following thermal treatment up to 400 and 700°C

Temperature (°C)	Pt Particle size (by TEM) (nm)	Pt particle size (by XRD) (nm)
No thermal treatment	<1	<1
400	18	19
700	20	10.5

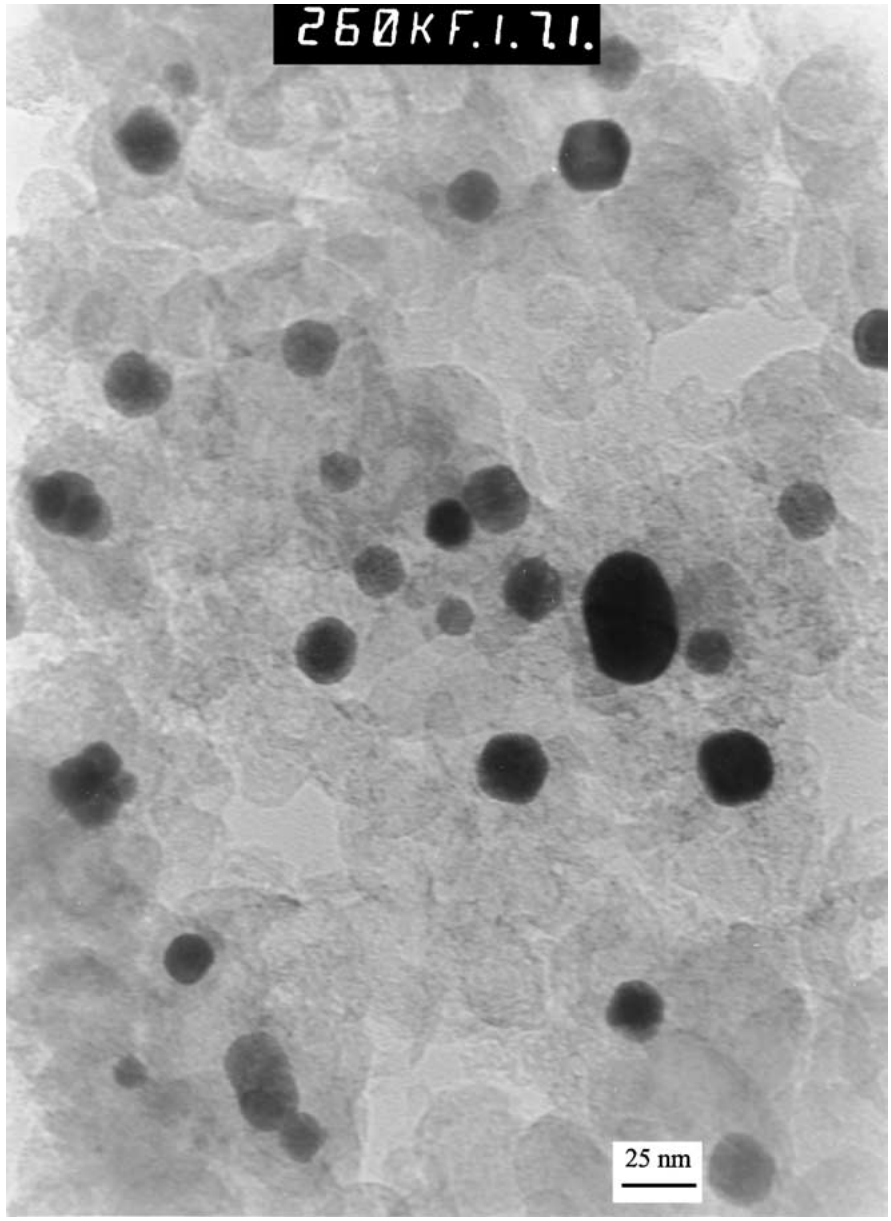

(c)

Figure 2 (*Continued.*)

be related to the presence of a secondary phase causing the broadening of XRD reflections. As we will report later, the catalyst thermally treated up to 700°C showed an anomalous behavior. Fig. 2 shows TEM micrographs following annealing up to 400 (Fig. 2b) and 700°C (Fig. 2c), respectively. The cubo-octahedral structure of the largest Pt particles can be seen. Fig. 5 shows the Pt particle size distribution from TEM analysis for samples annealed up to 400 (Fig. 5a) and 700°C (Fig. 5b), respectively. Particle size distribution of the catalyst thermally treated up to 400°C was symmetrical with respect to the maximum, while that of the sample treated up to 700°C showed a tail in the region of the large sizes. Going from 400 to 700°C, the particles with size <10 nm disappeared, while particles with size >40 nm were detected. The particle size of platinum supported on KJB following annealing up to 400°C, obtained from XRD measurements, was 18 nm, i.e. about the same value as that of platinum supported on VC. Then, the different support seems to affect the Pt particle size only before thermal treatment.

Regarding the thermocrystallization, we have considered as a crystallinity degree index of Pt particles the peak intensity ratio of the Pt [111] crystal face and the C[0015] reflection of the carbon. Fig. 6 shows the dependence of the Pt[111]/C[0015] intensity ratio vs. maximum temperature of the thermal treatment. A high increase of the crystallinity occurred in the temperature range 400–550°C, i.e. when the coalescence of Pt particles is almost completed. This indicates that grain growth and crystallite quality are independent events.

Following thermal treatment up to 350°C with different heating rate of 15°C/min and 45°C/min, XRD measurements (see Fig. 7) indicated the presence of Pt reflections with the same width at half height, but with increased intensity (peak intensity ratio 0.90 at heating rate 15°C/min, and 0.44 at heating rate 45°C/min), i.e. Pt particle size was the same, but the crystallinity increased with decreasing the heating rate. This means that the motion of Pt atoms on the support is faster than the motion of Pt atoms into the metal particle.

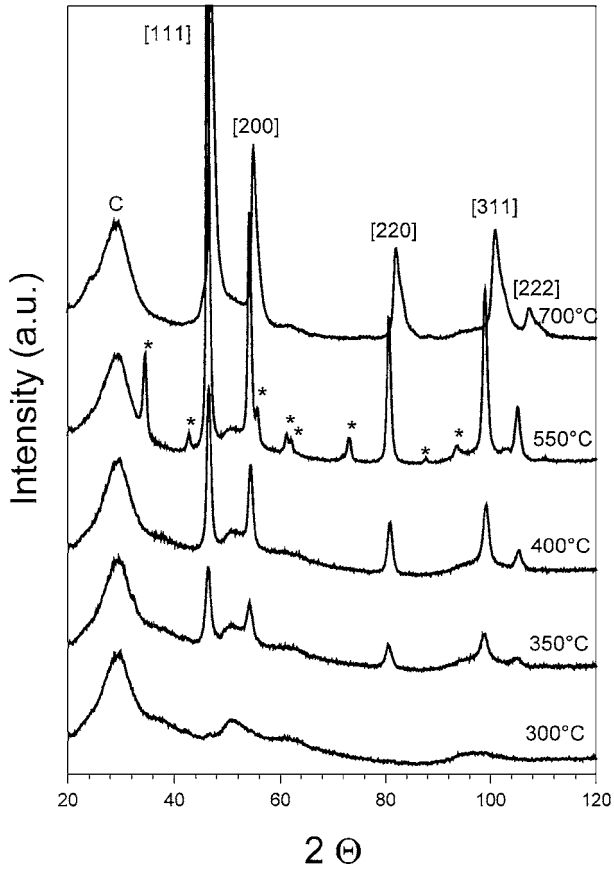

Figure 3 X-ray diffraction patterns of Pt/C on VC catalysts after annealing up to different temperatures. The asterisk ∗ in XRD pattern after annealing up to 550°C indicates PtS reflexions.

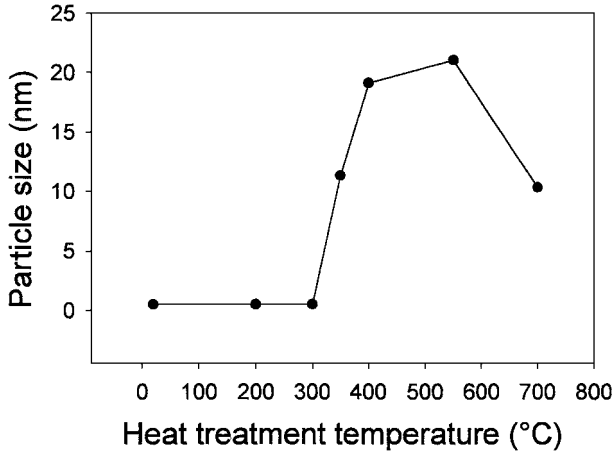

Figure 4 Dependence of platinum particle size of Pt/C on VC catalysts on the maximum temperature of the thermal treatment.

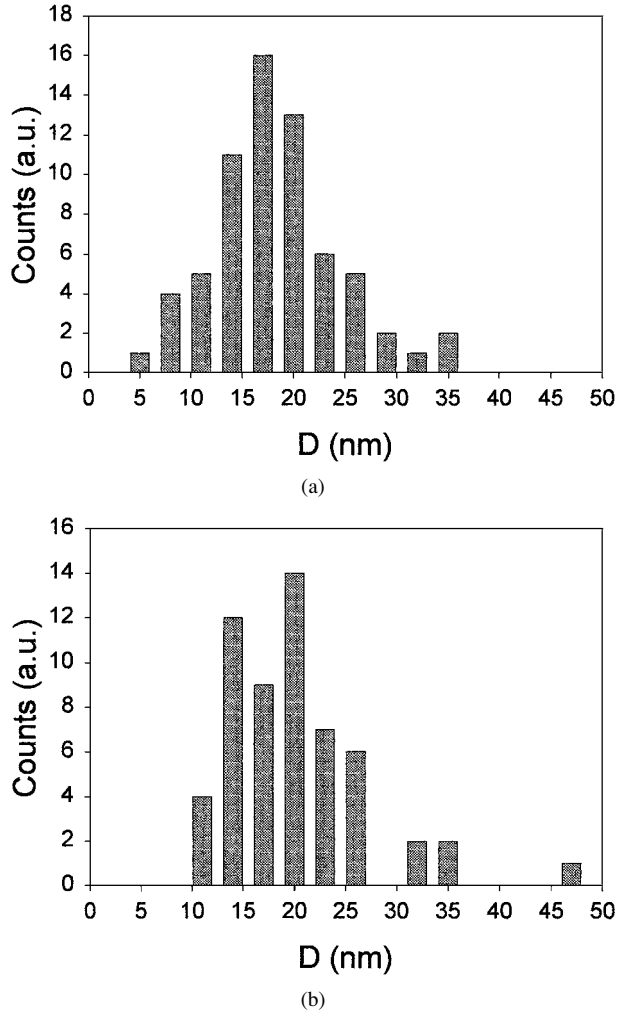

Figure 5 Size distribution of supported particles in Pt/C on VC catalysts after thermal treatment up to 400°C (a) and 700°C (b).

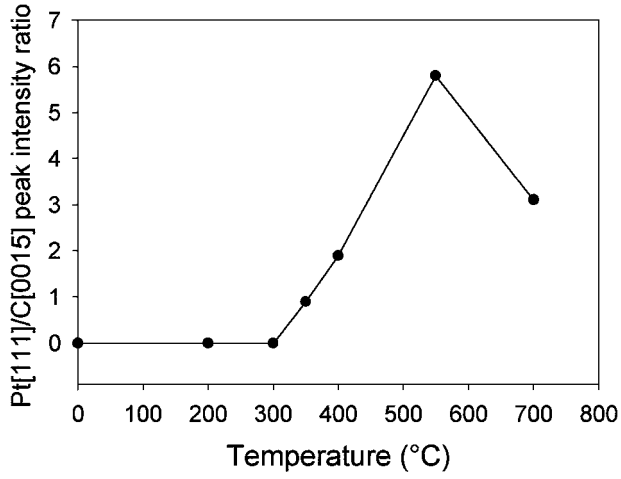

Figure 6 Pt[111]/C(0015) peak intensity ratio of Pt/C on VC catalysts as a function of the maximum temperature of the thermal treatment.

While after annealing up to 550°C regular fcc Pt and PtS phases were detected, following thermal treatment up to 700°C an anomalous fcc Pt phase was revealed by XRD analysis. The anomalous fcc Pt pattern of the sample thermally treated up to 700°C showed a large decrease of lattice constant (Fig. 8) and an increase of Pt[111]/Pt[220] peak intensity ratio (Fig. 9). These crystallographic anomalies and the decrease of the Pt[111]/C[0015] peak intensity ratio (Fig. 6) could be related to the concomitant decomposition of platinum sulfide formed during heating of the sample.

4. Conclusions

Pt/C catalysts were prepared using non-oxidized carbon support and a sulfur-based reducing agent. At relatively low temperature, in the range 300–400°C, Pt particle size grew from 1 to 20 nm. The crystallinity, on the other hand, increased in a remarkable way in the temperature range 400–550°C. The presence of sulfur affect the process of Pt/C formation in different ways, by chemical or physical interactions with platinum:

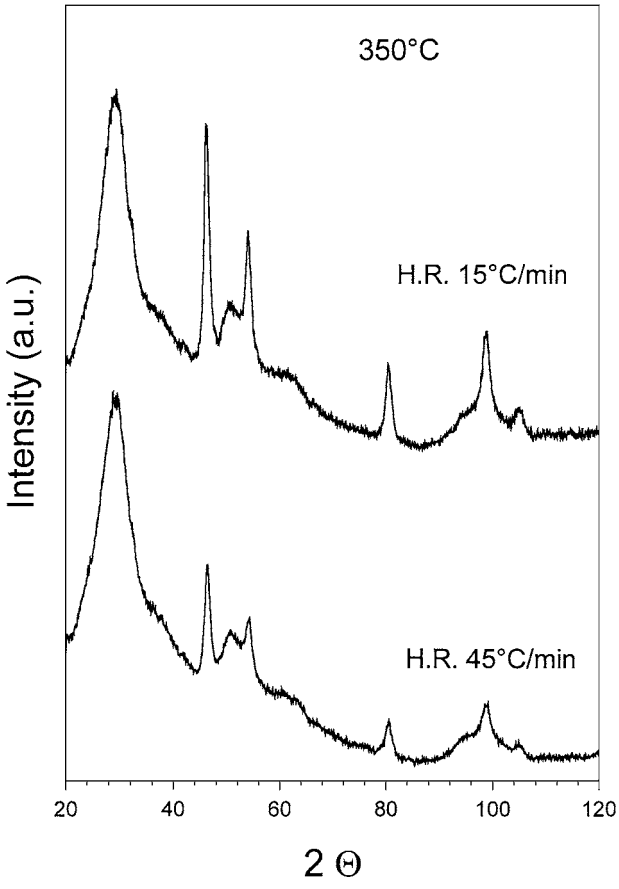

Figure 7 X-ray diffraction patterns of Pt/C on VC catalysts after annealing up to 350°C at heating rate 15°C/min and 45°C/min.

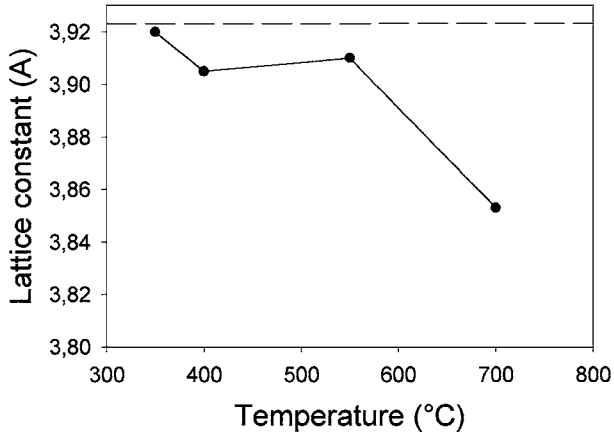

Figure 8 Dependence of Pt lattice constant (±0.001 Å) of Pt/C on VC catalysts on the maximum temperature of the thermal treatment. Dashed line: lattice constant value for unsupported platinum from JCPDS-International Centre for Diffraction Data (1998).

i) first, S acts a reducing and a nucleating agent;

ii) in the temperature range 300–400°C, sulfur supports the coalescence of Pt particles, enhancing Pt motion on the support by S bridge-bonding;

iii) during annealing up to 550°C chemical reaction of S and Pt takes place to give PtS;

iv) PtS decomposition at temperature higher than 550°C likely gives rise to the formation of a crystallographically anomalous fcc Pt.

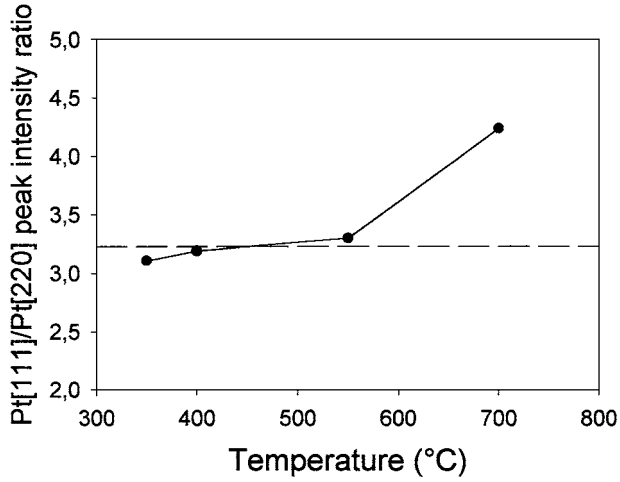

Figure 9 Dependence of Pt[111]/Pt[220] peak intensity ratio of Pt/C on VC catalyst on the maximum temperature of the thermal treatment. Dashed line: Pt[111]/Pt[220] value from JCPDS-International Centre for Diffraction Data (1998).

References

1. W. ROMANOWSKI, *Surf. Sci.* **18** (1969) 373.
2. J. KOLEHMAINEN, H. HAKKINEN and M. MANNINEN, *Z. Phys. D* **40** (1997) 306.
3. D. Y. SUN and X. G. GONG, *J. Phys. Cond. Matter* **9** (1997) 10555.
4. Y. MORO-OKA, Y. MORIKAWA and A. OZAKI, *J. Catal.* **7** (1967) 23.
5. M. L. SATTLER and P. N. ROSS, *Ultramicroscopy* **20** (1986) 21.
6. M. PEUCKERT, T. YONEDA, R. DALLA BETTA and M. BOUDART, *J. Electrochem, Soc.* **133** (1986) 944.
7. A. KABBABI, F. GLOAGUEN, F. ANDOLFATTO and R. DURAND, *J. Electroanal. Chem.* **373** (1994) 251.
8. A. C. C. TSEUNG and S. C. DHARA, *Electrochim, Acta* **20** (1975) 681.
9. A. HONJI, T. MORI, K. TAMURA and Y. HISHINUMA, *J. Electrochem. Soc.* **135** (1988) 355.
10. J. A. BETT, K. KINOSHITA and P. STONEHART, *J. Catal.* **41** (1976) 124.
11. *Idem., ibid.* **35** (1974) 307.
12. T. TORRE, A. S. ARICO', V. ALDERUCCI, V. ANTONUCCI and N. GIORDANO, *Appl. Catal. A* **114** (1994) 257.
13. C. HE, H. R. KUNZ and J. M. FENTON, *J. Electrochem. Soc.* **144** (1997) 970.
14. G. S. LODHA, S. PANDITA, A. GUPTA, R. V. NANDEDKAR and K. YAMASHITA, *Appl. Phys. A* **62** (1996) 29.
15. E. CZARAN, J. FINSTER and K. H. SCHNABEL, *Z. Anorg. Allg. Chem.* **443** (1978) 175.
16. H. E. VAN DAM and H. VAN BEKKUM, *J. Catal.* **131** (1991) 335.
17. S. R. DE MIGUEL, O. A. SCELZA, M. C. ROMAN-MARTINEZ, C. SALINAS-MARTINEZ, D. CAZORLA-AMOROS and A. LINARES-SOLANO, *Appl. Catal. A* **170** (1998) 93.
18. F. RODRIGUEZ-REINOSO, I. RODRIGUEZ-RAMOS, C. MORENO-CASTILLA, A. GUERRERO-RUIZ and J. D. LOPEZ-GONZALES, *J. Catal.* **99** (1986) 171.
19. K. TSURUMI, T. NAKAMURA and A. SATO, U.S. patent no. 4,956,331 (1990).
20. M. VAARKAMP, J. T. MILLER, F. S. MODICA, G. S. LANE and D. C. KONINGSBERGER, *J. Catal.* **138** (1992) 675.
21. S. C. ROY, P. A. CHRISTENSEN, A. HAMNETT, K. M. THOMAS and V. TRAPP, *J. Electrochem. Soc.* **143** (1996) 3073.

Received 31 October 2000
and accepted 28 August 2001